

Structures and properties of fluorinated amorphous carbon films

K. P. Huang, P. Lin, and H. C. Shih

Citation: [Journal of Applied Physics](#) **96**, 354 (2004); doi: 10.1063/1.1755849

View online: <http://dx.doi.org/10.1063/1.1755849>

View Table of Contents: <http://scitation.aip.org/content/aip/journal/jap/96/1?ver=pdfcov>

Published by the [AIP Publishing](#)

Articles you may be interested in

[Structural, optical, vibrational, and magnetic properties of sol-gel derived Ni doped ZnO nanoparticles](#)
J. Appl. Phys. **114**, 033912 (2013); 10.1063/1.4813868

[Electronic state modification in laser deposited amorphous carbon films by the inclusion of nitrogen](#)
J. Appl. Phys. **104**, 063701 (2008); 10.1063/1.2977718

[Comparative study of the effects of thermal treatment on the optical properties of hydrogenated amorphous silicon-oxycarbide](#)
J. Appl. Phys. **102**, 024302 (2007); 10.1063/1.2753572

[Spectroscopic properties of nitrogen doped hydrogenated amorphous carbon films grown by radio frequency plasma-enhanced chemical vapor deposition](#)
J. Appl. Phys. **89**, 7924 (2001); 10.1063/1.1371268

[Structural properties of fluorinated amorphous carbon films](#)
J. Appl. Phys. **87**, 621 (2000); 10.1063/1.371910



Re-register for Table of Content Alerts

Create a profile.



Sign up today!



Structures and properties of fluorinated amorphous carbon films

K. P. Huang and P. Lin

Department of Materials Science and Engineering, National Chiao-Tung University, Hsinchu, Taiwan 300, Republic of China

H. C. Shih^{a)}

Department of Materials Science and Engineering, National Tsing-Hua University, Hsinchu, Taiwan 300, Republic of China

(Received 22 September 2003; accepted 5 April 2004)

Fluorinated amorphous carbon (*a*-C:F) films were deposited by radio frequency bias assisted microwave plasma electron cyclotron resonance chemical vapor deposition with tetrafluoromethane (CF₄) and acetylene (C₂H₂) as precursors. The deposition process was performed at two flow ratios $R=0.90$ and $R=0.97$, where $R=CF_4/(CF_4+C_2H_2)$. The samples were annealed at 300 °C for 30 min. in a N₂ atmosphere. Both Fourier transform infrared and electron spectroscopy for chemical analyzer were used to characterize the *a*-C:F film chemical bond and fluorine concentration, respectively. A high resolution electron energy loss spectrometer was applied to detect the electronic structure. The higher CF₄ flow ratio ($R=0.97$) produced more *sp*³ linear structure, and it made the *a*-C:F film smoother and softer. A lifetime of around 0.34 μs and an energy gap of ~2.75 eV were observed in both the as-deposited and after annealing conditions. The short carriers lifetime in the *a*-C:F film made the photoluminescence peak blueshift. The annealing changed both the structure and composition of the *a*-C:F film. The type of fluorocarbon bond and electronic structure characterized the mechanical and physical properties of *a*-C:F film. © 2004 American Institute of Physics. [DOI: 10.1063/1.1755849]

I. INTRODUCTION

Future semiconductor devices in integrated circuits will soon be developed into a size as small as 0.07 μm. Therefore, a lower dielectric material should be used to lessen the degree of *RC* delay.^{1,2} Conventional low dielectric (low *k*) materials, like fluorinated silicate glass, methyl silsesquioxane, black diamond, etc., will not be able to meet the requirements of the future semiconductor devices. The new low *k* materials need to be electrically insulating and to have a low dielectric constant, chemical inertness, low moisture absorption, high thermal stability, high mechanical strength, and good adhesion to the neighboring layers. Recently, *a*-C:F films deposited at room temperature by plasma-assisted chemical-vapor-deposition (CVD) showed promising results.^{10,11,32} Hence, the *a*-C:F films have been considered as one potential candidate for intermetal dielectric materials applied in the next generation ultra-large scale integration devices.³⁻⁷

The *a*-C:F film with a low dielectric constant of about 1.5–2.0 can be deposited by various methods of plasma-based chemical vapor deposition.⁸⁻¹¹ The microwave plasma electron cyclotron resonance chemical vapor deposition (ECR-CVD) is one of the most promising deposition methods for producing the *a*-C:F films, because the ECR-CVD can generate a high density as well as a relatively large area of plasma. In addition, the depositing films have a fine surface planarity, good gap-filling capability, and uniformity as

well. The microwave plasma ECR-CVD system described in this article was used to produce reactive chemical species, and the rf bias assisted the precursor to impinge on the substrate, resulting in the deposition of the film. Both C₂H₂ and CF₄ were the precursors used for the synthesis of the *a*-C:F films. The C₂H₂ gas has a high C/H ratio, and could contribute enough carbon source to support a film network to increase the deposition rate.¹² The CF₄ gas has a high F/C ratio enough to supply sufficient fluorocarbons to raise the concentration of fluorine in the *a*-C:F film. The CF₄ plasma contains mainly CF₃⁺ ions, F neutrals, CF_{*n*} radicals, and negative ion species. Fluorine atoms control not only the concentration of CF_{*n*} radicals through the gas-phase reactions but also the surface reactions.¹³⁻¹⁷

In this article, we report on the chemical and physical properties of the fluorinated amorphous carbon film prepared by ECR-CVD, at two CF₄ flow ratios $R=0.90$ and $R=0.97$, where R is $CF_4/[CF_4+C_2H_2]$. This is to compare the difference between the as-deposited film and the film after annealing at 300 °C for 30 min. For this purpose we used the analytical instruments as follows: Fourier transform infrared absorption spectrophotometer (FTIR), electron spectroscopy for chemical analyzer (ESCA), high resolution electron energy loss spectrometer (HREELS), electron spin resonance spectrometer (EPR), photoluminescence spectrometer (PL), ultraviolet/visible spectrophotometer (UV/VI), field emission scanning electron microscope (FESEM), pulse laser spectrometer and atomic force microscope (AFM). The *sp*² content and the fluorine concentration would affect the photoluminescence lifetime, as well as energy band gap of the *a*-C:F films. With the rise of the temperature, the dangling

^{a)}Author to whom correspondence should be addressed; electronic mail: hcshih@mse.nthu.edu.tw

bond density increases, resulting from the growing numbers of unpaired spins in the defects in the films.

II. EXPERIMENT

Both CF_4 and C_2H_2 gases were mixed as precursors to deposit a -C:F films on p -type Si wafers by ECR-CVD. The plasma was produced by mixing both microwave (2.45 GHz) and radio frequency (13.56 MHz). The working pressure was fixed at 20 mtorr. Microwave power and rf bias were fixed at 600 W and -200 V, respectively. The C_2H_2 flow rate was varied from 3 to 10 sccm while CF_4 flow rate was fixed at 100 sccm. The plasma chemistry was examined, by the optical emission spectroscopy (OES), the Model ST121 from Princeton Instrument Inc. The a -C:F films were annealed in a pure nitrogen atmosphere at 300°C . The film thickness was measured by Hitachi 5000 type FESEM. The film morphology was observed with a Digital Instrument NS3a controller at a D3100 stage AFM while the hardness was measured by a Nano Scope E Hysitron 35 from Digital Instruments. The chemical bonds of the films were identified by FTIR and ESCA. The ESCA spectra were collected with an ESCA spectrometer using a Mg K x-ray anode operating at 400 W and 15 kV. A Gatan GIF 2000 HREELS was used to quantify the mass of sp^2 in the films. The dangling bonds of the a -C:F films were measured by EPR. The fluorescence was measured by the PL apparatus using a helium-cadmium (He-Cd) laser ($\lambda=325$ nm) as the excitation source. The optical band gap was characterized by UV/VI (HP 8453). An Excimer pulse laser ($\lambda=193$ nm) was used to evaluate photoluminescence lifetime.

III. RESULTS AND DISCUSSION

A. Plasma species and mechanical properties

The plasma composition depends on various chemical pathways in the plasma, as well as the plasma parameters, such as electron temperature, electron density, gas flow rate, and degree of ionization. To illustrate how these collisions could result in the radical production, Table I shows a set of reactions which is the possible sheath radical production in the C_2H_2 and CF_4 plasma.^{18–21,48} Figure 1 shows the optical emission spectra (OES) of the ECR-excited plasma. There are C_2 , C_3 , CF_2 , CH , F_2 , H_2 , and HF radical species, and C_2^- , F_2^+ , and HF^+ ionic species in the plasma.²² The C_2 radicals will construct the main skeleton of the a -C:F films, while the fluorine atoms will be replaced by hydrocarbons to form fluorocarbon bonds or HF bonds. Figure 2 shows the CF and CF_2 species found in the plasma with the spectra at wavelength range 200–300 nm. The F_2 , F_2^+ , CF , CF_2 , and CF_3 radicals are both sinks and sources²³ at the same time during the deposition of the a -C:F films. The spectrum of the $R=0.97$ plasma has higher intensity than that of the $R=0.90$ plasma. Therefore, it is clearly differentiated by the deposition rates of 55.5 and 5.83 nm/min obtained at $R=0.90$ and $R=0.97$, respectively. In addition, the higher gas flow ratio will supply more fluorine and fluorocarbon radicals, which would etch the weaker bonds and form the stronger sp^3 fluorocarbon bonds in the a -C:F films.

TABLE I. Primary electron collisions.

Product	Process	Apparent potential (eV)
H^+	$e^- + \text{C}_2\text{H}_2 \rightarrow \text{H}^+ + \text{H} + \text{C}_2 + 2e^-$ $\rightarrow \text{H}^+ + \text{H} + \text{CH} + \text{C} + 2e^-$	20.8
C^+	$e^- + \text{C}_2\text{H}_2 \rightarrow \text{C}^+ + 2\text{H} + \text{C} + 2e^-$	22.8
CH^+	$e^- + \text{C}_2\text{H}_2 \rightarrow \text{CH}^+ + \text{CH} + 2e^-$	24.5
C_2^+	$e^- + \text{C}_2\text{H}_2 \rightarrow \text{C}_2^+ + 2\text{H} + 2e^-$ $\rightarrow \text{C}_2^+ + \text{H}_2 + 2e^-$	22.2 23.8
C_2H^+	$e^- + \text{C}_2\text{H}_2 \rightarrow \text{C}_2\text{H}^+ + \text{H} + 2e^-$	18.2
C_2H_2^+	$e^- + \text{C}_2\text{H}_2 \rightarrow \text{C}_2\text{H}_2^+ + 2e^-$	17.8
C_2H_2^+	$e^- + \text{C}_2\text{H}_2^+ \rightarrow \text{C}_2\text{H} + \text{H}$	11.2
C_2H_2^+	$e^- + \text{C}_2\text{H}_2^+ \rightarrow \text{C}_2 + 2\text{H}$	-7.3
C_2H_2^+	$e^- + \text{C}_2\text{H}_2^+ \rightarrow 2\text{CH}$	-3.2
C_3H^+	$\text{CH}^+ + \text{C}_2\text{H}_2 \rightarrow \text{C}_3\text{H}^+ + \text{H}_2$	-3.1
C_3H_2^+	$\text{CH}^+ + \text{C}_2\text{H}_2 \rightarrow \text{C}_3\text{H}_2^+ + \text{H}$	22.9
C_4H_2^+	$\text{C}_2^+ + \text{C}_2\text{H}_2 \rightarrow \text{C}_4\text{H}^+ + \text{H}$	21.3
C_4H_2^+	$\text{C}_2^+ \text{H}_2^+ + \text{C}_2\text{H}_2 \rightarrow \text{C}_4\text{H}_2^+ + \text{H}_2$	19.2/22.5
C_4H_3^+	$\text{C}_2^+ \text{H}_2^+ + \text{C}_2\text{H}_2 \rightarrow \text{C}_4\text{H}_3^+ + \text{H}$	11.38
CF^+	$\text{CF}_3^+ + \text{CF}_4 \rightarrow \text{CF}^+ + 2\text{F}$	11.07
CF_3^+	$\text{CF}^+ + \text{CF}_4 \rightarrow \text{CF}_3^+ + \text{CF}_2$	8.08
CF_3^+	$\text{CF}_3^+ + \text{CF}_4 \rightarrow \text{CF}_4^+ + \text{CF}_3 \rightarrow \text{CF}_3^+ + \text{F} + \text{CF}_3$	0.3
CF_3^+	$\text{C}^+ + \text{CF}_4 \rightarrow \text{CF}_3^+ + \text{CF}$	6.2
CF_3^+	$e^- + \text{CF}_3^+ \rightarrow \text{CF}_2 + \text{F}$	-1.78
CF_3^+	$e^- + \text{CF}_3^+ \rightarrow \text{CF} + 2\text{F}$	-6.7
C^+	$\text{CF}^+ + \text{CF}_4 \rightarrow \text{C}^+ + \text{CF}_4 + \text{F}$	-2.3
		5.59

The topography of a -C:F films can be evaluated by AFM. The surface roughness (root mean square) of the a -C:F films is less than 0.8 nm, which assists to mechanical and electric applications. The relevant data is listed in Table II. The higher flow ratio ($R=0.97$) generates more linear fluorocarbon bonds, which will be annihilated after annealing. In contrast, the crosslinking bonds will be increased as the flow ratio is reduced. Consequently, the hardness of the a -C:F films depend on the fluorine content and the thermal

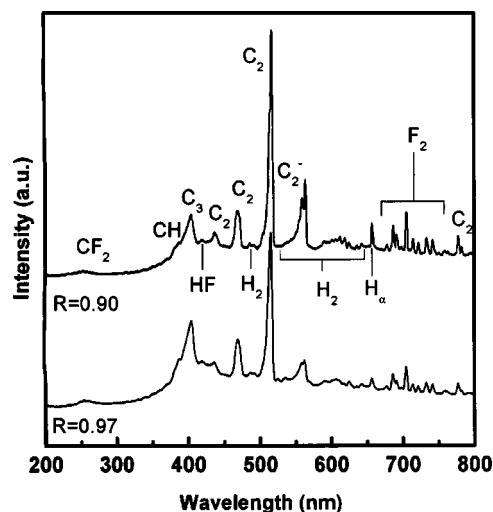


FIG. 1. Optical emission spectra obtained in C_2H_2 and CF_4 mixed gas discharge at 600 W source power -200 V rf bias, and 20 m Torr in the ECR-CVD.

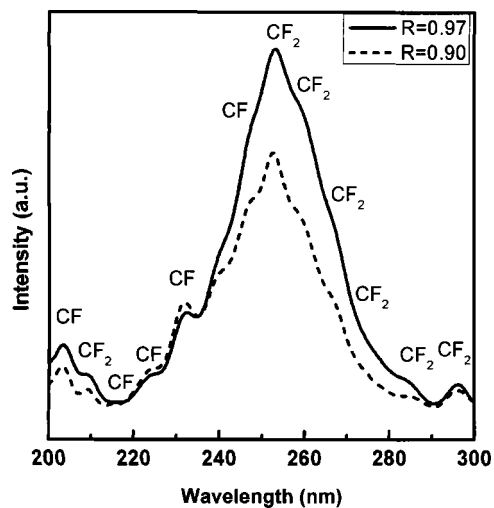


FIG. 2. Comparisons of the plasma optical emission spectra for $R=0.97$ and $R=0.90$.

treatment. Therefore the higher CF_4 flow ratio ($R=0.97$) produced more sp^3 linear structure, which made the a -C:F films smoother and softer.

B. Chemical bonding

FTIR is a very powerful instrument to detect the chemical structure of the a -C:F film, and it can give information for films as thick as of $\sim 1 \mu\text{m}$. Figure 3 shows the FTIR spectroscopy of the a -C:F films prepared at $R=0.97$ and $R=0.90$. There are only fluorocarbon bonds present at the vibrational absorbance peaks, without any hydrocarbon bonds on the spectrum. It indicates that all of the hydrogen atoms reacted with fluorine atoms during the plasma reactions, and consequently resulted in HF species in the plasma. The absorption peaks between carbon and fluorine in the FTIR are summarized in Table III.^{24–27} The obvious difference between $R=0.97$ and 0.90 is that the a -C:F films formed at $R=0.90$ do not have CF_3 980 cm^{-1} absorption peak. The major peaks of the a -C:F film ($R=0.97$) are $-CFCF_3$, CF_2 , and $C=CF$ stretches, whereas CF_2 and $C=CF$ stretches are the main peaks of the a -C:F films ($R=0.90$). The peak intensity of each as-deposited a -C:F film is stronger than that of each film after annealing (at 300°C). Moreover, Fig. 3 shows that the intensity of the peaks for after annealing a -C:F films is lower than that of the as-deposited film from 730 to 1350 cm^{-1} , which implies that there are plenty of CF_2 , CF_3 , and $CF-CF_3$ bonds that will be broken in the film after annealing. However, the spectra of the a -C:F films pre-

TABLE II. Comparisons of the properties of $R=0.90$ and 0.97 amorphous fluorinated carbon films as-deposited and after being annealed at 300°C .

	$sp^2\%$ (%)	Lifetime (μs)	E_g (eV)	Roughness (nm)	Hardness (GPa)
$R=0.90$ after annealed	41.5	0.46	2.48	0.79	0.59
$R=0.90$ as-deposited	39.3	0.43	2.51	0.78	0.74
$R=0.97$ after annealed	32.4	0.36	2.68	0.47	0.35
$R=0.97$ as-deposited	27.3	0.34	2.75	0.57	0.44

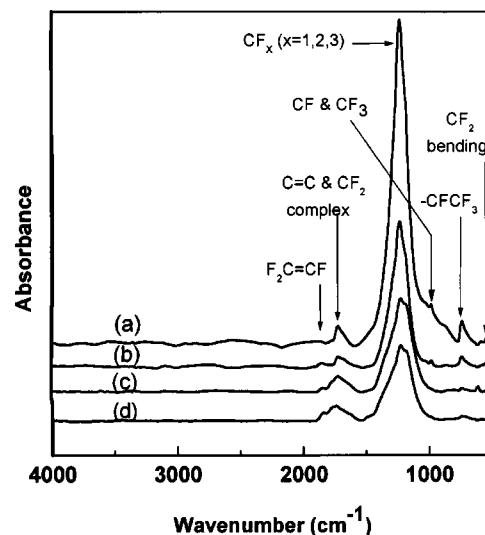


FIG. 3. FTIR spectroscopy of the a -C:F film, (a) as-deposited at $R=0.97$, (b) after being annealed at $R=0.97$, (c) as-deposited at $R=0.90$, (d) after being annealed at $R=0.90$.

pared at $R=0.90$ are almost the same in both conditions: as-deposited and after annealing. Hence the structure of the $R=0.90$ film is more stable than the one prepared at $R=0.97$.

C. ESCA analysis

ESCA is another powerful instrument for detecting the chemical structure of the a -C:F films, and is also a surface sensitive instrument providing the local chemical bonds of only the first $\sim 50 \text{ \AA}$ of the thin film. The $C 1s$ spectrum of a -C:F film could be deconvoluted into five Gaussian peaks corresponding to CF_3 (293.2 eV), CF_2 (290.95 eV), CF (288.8 eV), $C-CF_x$ (286.5 eV), and $C-C$ or $C-H$ (284.9 eV), as shown in Fig. 4. The absolute binding energies of CF_3 , CF_2 , CF , $C-CF_x$ and $C-C$ fall within the range, as listed in the published literature,^{28–34} valuing from 292.6 to 294 , 290.3 to 292 , 287.8 to 289.3 , 285.5 to 287.3 , and 283.4 to 285 eV , respectively. From the deconvolution of the $C 1s$

TABLE III. Summary of FT-IR absorption peaks.

Wave number (cm^{-1})	Assignment
505	CF_2 rocking
553	CF_2 bending
635	CF_2 wagging
730–745	$CF-CF_3$
980	CF_3
1030 and 1070	CF
1120–1350	CF_3 group
1160	CF_2 symmetric stretch
1220 and 1450	CF_2 asymmetric stretch
1300–1340	$CF=CF_2$
1325–1365	CF_3CF_2
1340	CF stretch
1608–1700	$C=CF$ stretch
1700	$C=C$ stretch
1720	$F_2C=C<$
1860	$F_2C=CF$

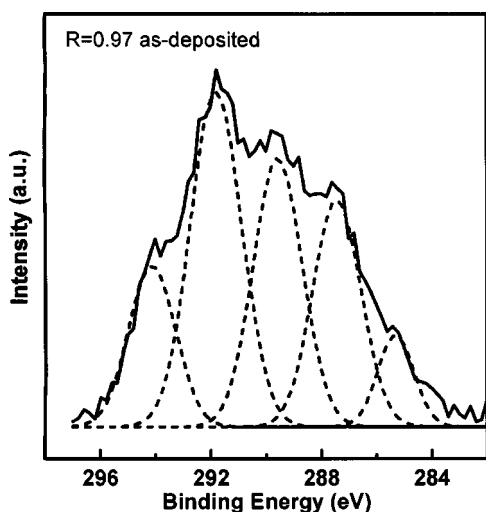


FIG. 4. Deconvoluted C 1s spectrum of a-C:F film at R=0.97 as-deposited obtained by ESCA analysis.

spectrum, fluorine-to-carbon ratios (F/C) can easily be calculated by the integrated intensity of the various components of the C 1s spectrum,³⁵ according to

$$F/C = (3I_{CF_3} + 2I_{CF_2} + I_{CF}) / I_{C\ 1s}$$

where I_{bond} is the photoemission intensity (i.e., area under each Gaussian curve) originating from a specific bond. Figure 5 and Table IV show the results from the C 1s spectrum deconvolution. The fluorine concentration of the R = 0.97 a-C:F film is higher than that of the R = 0.90 film, and the main peak of the R = 0.97 a-C:F film is the CF₂ bond in both as-deposited and after annealing conditions. In contrast to the CF₂ bond of the R = 0.97 a-C:F film, the C-CF_x bond of the R = 0.90 film is the main peak in the as-deposited condition and the C-C bond is the main peak after annealing. The mass of the C-C bond falls as the CF₄ flow ratio rises. When we increase the flow ratio R, the CF₂ concentration will grow significantly. Evidently, the C 1s deconvolution varies in both R = 0.97 and 0.90 films in as-deposited

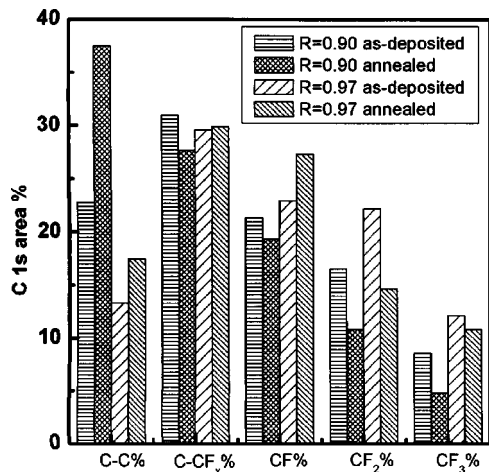


FIG. 5. Deconvolution result of the a-C:F film C 1s spectrum for R = 0.97 and R = 0.90 at as-deposited and after being annealed obtained by ESCA analysis.

TABLE IV. ESCA chemical composition (at. %) of the a-C:F films as-deposited and after being annealed at 300 °C.

CF ₄ Flow ratio	C-C	C-CF _x	C-F ₁	CF ₂	CF ₃	F%
R = 0.97 (as-deposited)	6.3	20.9	25.3	32.9	14.5	57.4
R = 0.97 (after annealed)	9.4	25.4	23.1	28.8	13.3	54.7
R = 0.90 (as-deposited)	22.7	31.0	21.3	16.5	8.5	44.4
R = 0.90 (after annealed)	37.5	27.6	19.3	10.8	4.8	35.6

and after-annealed conditions. The peak areas for C-CF_x, CF, CF₂, and CF₃ shrink with the R = 0.90 a-C:F film being annealed, but the amount of the C-C peak area increases relatively. The peak areas for CF, CF₂, and CF₃ decrease when the R = 0.97 a-C:F film is annealed, but the C-C and C-CF_x peak areas increase relatively. This is because the a-C:F film will break a lot of weaker bonds in the a-C:F film, and release fluorocarbon molecules during annealing. Consequently, the fluorine concentration will decrease after the a-C:F film is annealed.

D. HREELS analysis

The HREELS is the most reliable method for quantifying the sp² bond fraction. The a-C:F films often comprise a combination of two types of bonding: sp³ and sp² type hybridizations. The bonding types can be analyzed by studying the K-shell electron-energy-loss (EELS) spectrum of C 1s. Figure 6 shows the HREELS spectra in the carbon K-edge region after the background is removed. The steep rise at 287.4 eV in the diamond spectrum of the 100% sp³ bonds corresponds to the onset of the 1s → σ* transitions, and the peak position at about 285 eV corresponds to the dangling bonds on the surface and/or to the defects in the crystal. The graphite spectrum, which is 100% sp² bonds structure, shows a clear peak at 285 eV and a steep rise at 289.4 eV

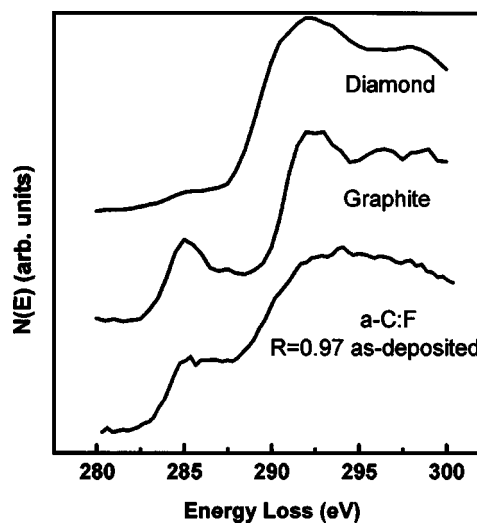


FIG. 6. Comparisons of the HREELS spectra in the carbon K-edge region.

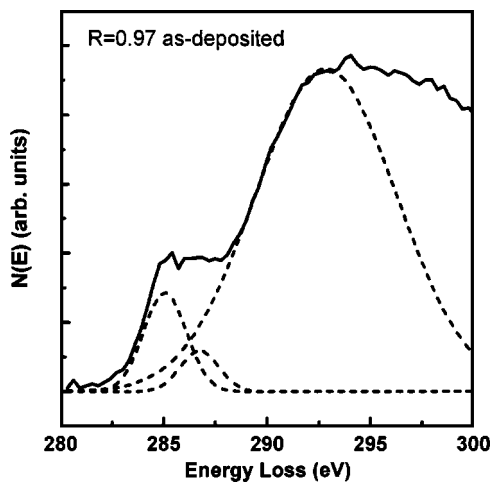


FIG. 7. Carbon K -ionization edge spectra obtained from $R=0.97$ as-deposited. The fit obtained when using three Gaussian peaks centered at 285, 287, and 293 eV.

corresponding to the $1s \rightarrow \pi^*$ and to the onset of $1s \rightarrow \sigma^*$ transitions, respectively.^{36,37} The a -C:F film spectrum almost matches a diamondlike carbon (a -C or a -C:H) one.^{36–38} Moreover, both the fluorinated amorphous carbon and diamondlike carbon films are sp^3 and sp^2 mixed structures.

The method for qualifying the sp^2 bonding fraction in the a -C:F films from the electron-energy-loss spectra is described by Berger *et al.*³⁶ Here, the area under the $1s \rightarrow \pi^*$ peak of the a -C:F film is normalized to a energy window, referring to an equivalent ratio for graphite, which has 100% sp^2 bonding. The mathematical principle for quantifying the edge is to obtain a ratio of the two areas, one of which is the standard, as shown in the following formula:

$$f = \frac{I_g \pi^* I_u(\Delta E)}{I_u \pi^* I_g(\Delta E)} \quad (1)$$

where f is the ratio between the two π^* peaks, I_{π^*} is the integral $1s \rightarrow \pi^*$ transition of graphite, and $I(\Delta E)$ is the integrated counts for normalizing the energy windows. The superscripts g and u denote the graphite and unknown spectra respectively.

Figure 7 shows the carbon K -edge fitting of the $R=0.97$ as-deposited amorphous carbon films. There are three Gaussian peaks in the spectra which are centered at 285, 287, and 293 eV, and these peaks indicate the $1s \rightarrow \pi^*$ transition, the molecular transition, and $1s \rightarrow \sigma^*$ transitions respectively.^{36,39–41} The quantity of the sp^2 bonds in the a -C:F film, estimated according to Eq. (1), is listed in Table II. The sp^2 fraction decreases with an increasing CF_4 flow ratio. At a higher CF_4 flow ratio, more fluorine atoms are supplied, each of which in turn can be bonded with carbon. This reaction is similar to the H atom with its ability to stabilize the dangling bond in amorphous carbons.⁴² It is generally believed that the fluorine atom helps to the increase of the sp^3 bonding components in the a -C:F film. Furthermore, the sp^3 fraction decreases when the a -C:F film is annealed. The sp^3 bonds of the diamondlike carbon belong to a metastable phase,^{43–45} so the magnitude of sp^2 bonds of the a -C:F film will be enlarged after annealing.

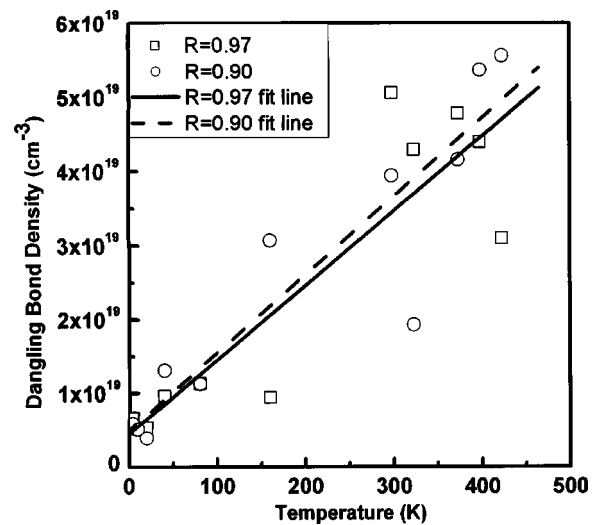


FIG. 8. Dangling bond density of the a -C:F films at $R=0.97$ and $R=0.90$ as-deposited.

When comparing the mechanical properties, we find that the $R=0.97$ films are smoother and softer than the $R=0.90$ films. Therefore we believe that the sp^3 bonds in the film must be in a linear form rather than in the network one found in the a -C:F films. With such large quantities of sp^3 bonds in diamondlike films, the hardness is usually over 20 GPa.^{47–49}

E. Dangling bond

The dangling bond defects, which give rise to states around the Fermi level, are important in electronic materials as they usually control the recombination of carriers. The states can be either diamagnetic or paramagnetic.⁴¹ The density of paramagnetic defects can be easily measured by EPR. The range of dangling bond densities of a -C:F films at $R=0.97$ and $R=0.90$ as-deposited is $\sim 2 \times 10^{19} - 5 \times 10^{20}$ spins/cm³ from 4 to 423 K. However, after being normalized by the Curie's law, the range of dangling bond densities is $\sim 5.5 \times 10^{18} - 5.5 \times 10^{19}$ as shown in Fig. 8. The hopping rate of a dangling bond electron is lower at a low temperature.⁴⁶ As the temperature rises, the unpaired spins will increase considerably due to the electron hopping from the defects. Furthermore, numerous nanovoids exist in the a -C:F film.¹¹ These nanovoids are supposed to enhance dangling bond density with the rise of temperature. The higher fluorine concentration has lower dangling bond density in the a -C:F film, which means that the fluorine atoms and ions can easily react with the dangling bonds of the carbon frame during the CVD deposition. In addition, after annealing the a -C:F films, the leakage current at a higher flow ratio of a -C:F films would be less than that at a lower flow ratio.¹¹

F. Optical characteristics

The a -C:F film has a broadband luminescence characteristic of an amorphous semiconductor with broad band tails. Figure 9 shows PL spectra for $R=0.97$ and $R=0.90$ a -C:F films in both as-deposited and after annealing conditions. The PL peak band is like rough Gaussian peak, and changes

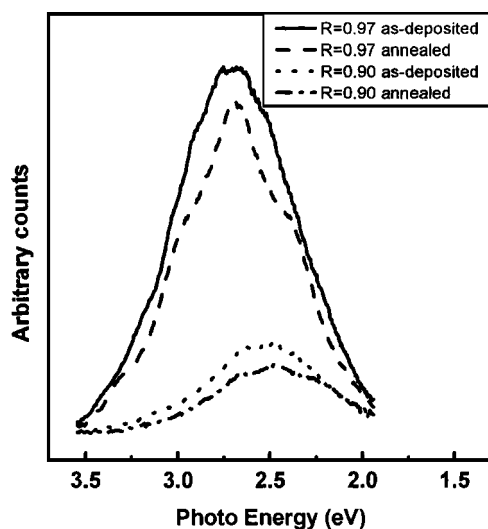


FIG. 9. PL spectra produced at $R=0.97$ and at $R=0.90$ of a -C:F films for both as-deposited and after being annealed at 300°C .

with the CF_4 flow ratio. The PL peak site tends to be blue-shifted as the fluorine concentration increases. It is also noticed that annealing helps to reduce the full width at half maximum of the PL spectra. The broad spectrum results from structural disorder of the a -C:F film. Fluorinated amorphous carbon films after the annealing treatment will be structurally relaxed because the disappearance of electron-hole pairs lower the probability of the radiative recombination.⁴¹ The higher fluorine concentration enhances a higher sp^3 content in the film, so the as-deposited $R=0.97$ film tends to blueshifted.

The spectrophotometry of the UV/VI bands of the a -C:F films is plotted in Fig. 10. The optical band gap listed in Table II was determined by the Tauc mode.⁵⁰ Since the C-F bond energy (102 kcal/mole) is higher than the C-C bond energy (80 kcal/mole), the greater number of fluorocarbon bonds in the a -C:F film produced at higher CF_4 flow ratios gives rise to a higher optical band gap. In addition, the C=C bonds or graphitelike sp^2 structures will lower the optical

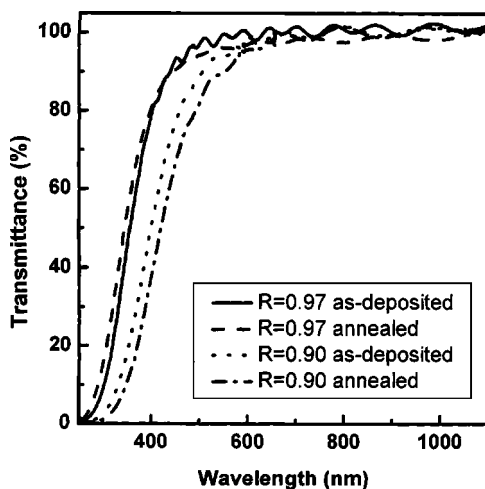


FIG. 10. UV/VI spectra of both $R=0.97$ and $R=0.90$ of the a -C:F films as-deposited and after being annealed at 300°C .

band gap,⁵¹ so the optical band gap of the as-deposited a -C:F film is larger than the one after annealing. This is also the reason why the $R=0.97$ film has less blueshift than the $R=0.90$ film. The optical properties are closely correlated to the amount of fluorine incorporated into the films. The increase in the optical band gap energy indicates that the fluorine incorporated into the a -C:F film has modified the chemical structure of the film towards the higher sp^3 bonding fraction.⁵¹ These properties are similar to those of hydrogenated amorphous carbon.^{48,52,53}

Excimer pulse laser spectrometer was used to measure the lifetime (τ). The results are listed in Table II. The photoluminescence lifetime is directly proportional to both fluorine concentration and $sp^2\%$ for as-deposited films and after annealing. The lifetime is longer in a -C:F (10^{-7} s) than in a -C:H (10^{-8} s),^{54,55} but is much shorter than in a -Si:H (10^{-3} s).^{56,57} The short lifetime of carriers reduces their energy relaxation into lower energy states and then increases the average energy of carriers in the band tail state.⁵⁸ The short photoluminescence lifetime causes a blueshift of the lowest energy accessible to carriers for radiative recombination in the band tail state.⁵⁹ Therefore, we can observe the pronounced blueshift of the PL peak in a -C:F film, because of the short carrier lifetime.

IV. CONCLUSIONS

The sp^3 bond ratio can be increased by the fluorine concentration through an increase in the fluorocarbon flow ratio. The FTIR and ESCA results reveal that the structure of the a -C:F films prepared at various CF_4 flow ratios are different. Furthermore, the result of EELS reveals that annealing the films can increase the carbon double bond structure in the a -C:F films. The higher CF_4 flow ratios produce more sp^3 linear structure, and make the a -C:F film smoother and softer. There is a lot of structural variation after annealing; therefore, the electrical and optical properties of the a -C:F films are different from these of the as-deposited films. The higher fluorine concentration will promote a greater number of fluorine carbon bonds in the film and therefore produce a higher energy band gap. Furthermore, annealing will induce the sp^2 structure in the a -C:F film, which will extend the photoluminescence lifetime. The short carriers lifetime in the a -C:F film makes PL peak blue-shift.

ACKNOWLEDGMENTS

This work is supported by Dr. S. Roth, Max-Planck Institute Stuttgart, and the National Science Council of the Republic of China under No. NSC 91-2219-E009-028.

¹M. T. Bohr, Solid State Technol. **39**, 105 (1996).

²Y. Matsubara, K. Kishimoto, K. Endo, M. Iguchi, T. Tasumi, H. Gomi, T. Horiuchi, E. Tzou, M. Xi, L. Y. Cheng, D. Tribula, and F. Moghadam, IEEE IEDM **31**, 841 (1998).

³J. A. Theil, F. Mertz, M. Yairi, K. Seaward, G. Ray, and G. Kooi, in *Low-Dielectric Constant Materials*, edited by C. Case, P. Kohl, T. Kikkawa, and W. W. Lee, Mater. Res. Soc. Symp. Proc. No. 476 (Materials Research Society, Pittsburgh, 1997), p. 31.

⁴T. W. Mountsier, J. A. Saquels, and R. S. Swope, in *Low-Dielectric Constant Materials*, edited by C. Chiang, P. S. Ho, T. M. Lu, and J. T.

- Wetzel, Mater. Res. Soc. Symp. Proc. No. 511 (Materials Research Society, Pittsburgh, 1998), p. 259.
- ⁵K. Endo, T. Tatsumi, Y. Matsubara, and T. Horiuchi, Jpn. J. Appl. Phys., Part 1 **37**, 1809 (1998).
- ⁶N. H. Hendricks, Mater. Res. Soc. Symp. Proc. **443**, 3 (1997).
- ⁷T. W. Mountsier and D. Kumar, in *Low-Dielectric Constant Materials*, edited by A. Lagendijk, H. Treichel, K. J. Uram, and A. C. Jones, Mater. Res. Soc. Symp. Proc. No. 443 (Materials Research Society, Pittsburgh, 1998), p. 41.
- ⁸K. Endo and T. Tatsumi, J. Appl. Phys. **78**, 1370 (1995).
- ⁹K. Endo, T. Tatsumi, Y. Matsubara, and T. Horiuchi, Jpn. J. Appl. Phys., Part 1 **37**, 1809 (1998).
- ¹⁰H. Yokomichi, T. Hayashi, T. Amano, and A. Masuda, J. Non-Cryst. Solids **227–230**, 641 (1998).
- ¹¹K. P. Huang, P. Lin, and H. C. Shih, Jpn. J. Appl. Phys., Part 1 **42**, 3598 (2003).
- ¹²P. S. Andry, P. W. Pastel, and W. J. Varhue, J. Mater. Res. **11**, 221 (1996).
- ¹³G. Chuge and J. P. Booth, J. Appl. Phys. **85**, 3952 (1999).
- ¹⁴W. Schwarzenbach, G. Cunge, and J. P. Booth, J. Appl. Phys. **85**, 7562 (1999).
- ¹⁵K. Teii, M. Hori, M. Ito, T. Goto, and N. Ishii, J. Vac. Sci. Technol. A **18**, 1 (2000).
- ¹⁶L. G. Jacobsohn, D. F. Franceschini, M. E. H. Maia da Costa, and F. L. Freire, Jr., J. Vac. Sci. Technol. A **18**, 2230 (2000).
- ¹⁷K. Sasaki, H. Furukawa, K. Kadota, and C. Suzuki, J. Appl. Phys. **88**, 5585 (2000).
- ¹⁸M. Stacey, *Advances in Fluorine Chemistry* (Butterworths, Washington, 1965).
- ¹⁹F. H. Field and J. L. Franklin, *Electron Impact Phenomena and the Properties of Gaseous Ions* (Academic Press, New York, 1970).
- ²⁰R. J. M. N. Snijkers, Ph.D. Thesis, Eindhoven University of Technology, The Netherlands, 1993.
- ²¹J. W. A. M. Gielen, M. C. M. van de Sanden, and D. C. Schram, Thin Solid Films **271**, 56 (1995).
- ²²R. W. B. Pearse and A. G. Gaydon, *The Identification of Molecular Spectra*, 4th Ed. (Wiley, New York, 1976).
- ²³Da Zhang and M. J. Kushner, J. Vac. Sci. Technol. A **18**, 2661 (2000).
- ²⁴Norman B. Colthup, Lawrence H. Daly, and Stephen E. Wiberley, *Introduction to Infrared and Raman Spectroscopy*, 3rd Ed. (Academic Press, Boston, 1990), Chap. 12.
- ²⁵M. Inayoshi, M. Hori, T. Goto, M. Hiramatsu, M. Nawata, and S. Hattori, J. Vac. Sci. Technol. A **14**, 1981 (1996).
- ²⁶D. C. Marra and E. S. Aydil, J. Vac. Sci. Technol. A **15**, 2508 (1997).
- ²⁷H. Yokomichi and A. Masuda, Vacuum **59**, 771 (2000).
- ²⁸M. A. Butler, R. J. Buss, and A. Galuska, J. Appl. Phys. **70**, 2326 (1991).
- ²⁹K. Endo and T. Tatsumi, J. Appl. Phys. **78**, 1370 (1995).
- ³⁰A. M. Hynes, M. J. Shenton, and J. P. S. Badyal, Macromolecules **29**, 4220 (1996).
- ³¹S. F. Durrant, S. G. C. Castro, L. E. Bolívar-Marinez, D. S. Galvão, and M. A. B. de Moraes, Thin Solid Films **304**, 149 (1997).
- ³²Y. Ma, H. Yang, J. Guo, C. Sathe, A. Agui, and J. Nordgren, Appl. Phys. Lett. **72**, 3353 (1998).
- ³³M. Schaepekens, T. E. F. M. Standaert, N. R. Rueger, P. G. M. Sebel, G. S. Oehrlein, and J. M. Cook, J. Vac. Sci. Technol. A **17**, 26 (1999).
- ³⁴S. Agraharam, D. W. Hess, P. A. Kohl, and S. A. Bidstrup, J. Vac. Sci. Technol. A **17**, 3265 (1999).
- ³⁵R. d'Agostino, editor, *Plasma Deposition, Treatment, and Etching of Polymers* (Academic Press, Boston, 1990), p. 146.
- ³⁶S. D. Berger, D. R. McKenzie, and P. J. Martin, Philos. Mag. Lett. **57**, 285 (1988).
- ³⁷R. G. Pregliasco, G. Zampieri, H. Huck, E. B. Halac, M. A. R. de Benyacar, and R. Righini, Appl. Surf. Sci. **103**, 261 (1996).
- ³⁸P. J. Fallon, V. S. Veerasamy, C. A. Davis, J. Robertson, G. A. J. Amarantunga, W. I. Milne, and J. Koskinen, Phys. Rev. B **48**, 4777 (1993).
- ³⁹A. P. Hitchcock, D. C. Newbury, I. Ishii, J. Stöhr, J. A. Horsley, R. D. Redwing, A. L. Johnson, and F. Sette, J. Chem. Phys. **85**, 4849 (1986).
- ⁴⁰R. McLaren, S. A. C. Clark, I. Ishii, and A. P. Hitchcock, Phys. Rev. A **36**, 1683 (1987).
- ⁴¹S. R. P. Silva, J. Robertson, Rulsli, G. A. J. Amarantunga, and J. Schwan, Philos. Mag. B **74**, 369 (1996).
- ⁴²H. Efstathiadis, Z. Akkerman, and F. W. Smith, J. Appl. Phys. **79**, 2954 (1996).
- ⁴³D. R. McKenzie, D. Muller, and B. A. Pailthorpe, Phys. Rev. Lett. **67**, 773 (1991).
- ⁴⁴D. R. McKenzie, J. Vac. Sci. Technol. B **11**, 1928 (1993).
- ⁴⁵J. Robertson, Diamond Relat. Mater. **3**, 361 (1994).
- ⁴⁶H. Yokomichi and K. Morigaki, J. Non-Cryst. Solids **266–269**, 797 (2000).
- ⁴⁷M. Weiler, J. Roberson, S. Sattel, V. S. Veerasamy, K. Jung, and H. Ehrhardt, Diamond Relat. Mater. **4**, 304 (1995).
- ⁴⁸M. Weiler, S. Sattel, T. Giessen, K. Jung, H. Ehrhardt, V. S. Veerasamy, and J. Robertson, Phys. Rev. B **53**, 1594 (1996).
- ⁴⁹R. G. Lacerda, F. C. Marques, and Freire, Jr., Diamond Relat. Mater. **8**, 495 (1999).
- ⁵⁰Richard Zallen, *The Physics of Amorphous Solids*, 2nd Ed. (Wiley, New York, 1998).
- ⁵¹A. Weber, R. Pöckelmann, and C.-P. Klages, J. Vac. Sci. Technol. A **16**, 2120 (1998).
- ⁵²Th. Frauenheim, G. Jungnickel, U. Stephan, P. Blaudeck, S. Deutschmann, M. Weriler, S. Sattel, K. Jung, and H. Ehrhardt, Phys. Rev. B **50**, 7940 (1994).
- ⁵³M. Hakovirta, X. M. He, and M. Nastasi, J. Appl. Phys. **88**, 1456 (2000).
- ⁵⁴Rulsli, Gehan A. J. Amarantunga, and J. Roberson, Phys. Rev. B **53**, 16306 (1996).
- ⁵⁵W. Lormes, M. Hundhausen, and L. Ley, J. Non-Cryst. Solids **227–230**, 570 (1998).
- ⁵⁶W. Siebert, R. Carius, W. Fuhs, and K. Jahn, Phys. Status Solidi B **140**, 311 (1987).
- ⁵⁷S. Liedtke, K. Lips, M. Bort, K. Jahn, and W. Fuhs, J. Non-Cryst. Solids **114**, 522 (1989).
- ⁵⁸Y. Kanemitsu, M. Liboshi, and T. Kushida, Appl. Phys. Lett. **76**, 2200 (2000).
- ⁵⁹M. J. Estes and G. Moddel, Appl. Phys. Lett. **68**, 1814 (1996).